Nov 7th, 12:00 AM - Nov 8th, 12:00 AM

Proposal to Improve the DSM Design of Cold-Formed Steel Angle Columns: Need, Background, Quality Assessment and Illustration

Pedro Borges Dinis

Dinar Camotim

Wei-Wen Yu International Specialty Conference on Cold-Formed Steel Structures
St. Louis, Missouri, U.S.A., November 7 & 8, 2018

Proposal to Improve the DSM Design of Cold-Formed Steel Angle Columns: Need, Background, Quality Assessment and Illustration

Pedro Borges Dinis[1] and Dinar Camotim[1]

Abstract

This paper presents a proposal for the codification of an efficient design approach, based on the Direct Strength Method (DSM), for cold-formed steel equal-leg angle columns with short-to-intermediate lengths, *i.e.*, those buckling in flexural-torsional modes. Initially, the available experimental failure load data, comprising fixed-ended and pin-ended ("cylindrical hinges") columns with several geometries (cross-section dimensions and lengths) and tested by various researchers, are collected and used to show that the currently codified DSM design provisions are not able to handle adequately short-to-intermediate angle columns and that a specific DSM-based design approach is needed to estimate the failure loads of such columns. Then, the paper presents a brief overview of the structural reasoning behind the DSM-based design approach proposed by Dinis & Camotim (2015, 2016). Next, the quality (accuracy and reliability) of the failure load estimates obtained with this design approach is assessed through the comparison with the above experimental failure load data and also a fairly large number of numerical failure loads. This merit assessment includes the determination of the LRFD resistance factors concerning the failure-to-predicted load ratios – it is shown that the value recommended, for compression members, by the North American Specification (AISI 2016), ϕ_c=0.85, can also be adopted for short-to-intermediate angle columns designed with this DSM-based approach. Finally, the paper presents and discusses a few numerical examples, which illustrate the application of the proposed design approach and provide evidence of its advantages and benefits, when compared with the currently codified one.

1. Introduction

The geometrical simplicity of angles can only be matched by their complex structural behavior, a feature that is responsible for the fact that the most recent North American Specification (NAS) for the Design of Cold-Formed Steel Structural Members (AISI 2016) does not cover adequately the design of short-to-intermediate equal-leg angle columns (*i.e.*, those buckling in flexural-torsional modes) by means of the Direct Strength

[1] CERIS, ICIST, DECivil, Instituto Superior Técnico, Universidade de Lisboa, Lisbon, Portugal.

Method (DSM – *e.g.*, Schafer 2008, Camotim *et al*. 2016). Indeed, up until 2012 angle columns were not pre-qualified to be designed using the DSM (AISI 2012). Although the concept of pre-qualification was removed (AISI 2016), no novel provisions or guidelines for the DSM design of angle columns were added to the specification. Thus, it is only viable to use the currently codified DSM strength curve against local-global interactive failures to predict the intermediate angle column failure loads[2] – however, as clearly shown in this work, the corresponding failure-to-predicted load ratios, concerning the available experimental and/or numerical failure loads, invariably lead to LFRD (Load and Resistance Factor Design) resistance factors below the value recommended for compression members (ϕ_c=0.85). This stems from the fact that these columns buckle in flexural-torsional modes, associated with an almost horizontal "critical load plateau" of the corresponding "signature" curve P_{cr} vs. L (Fig. 1 shows typical fixed-ended and pin-ended angle column curves[3]) – L is the column length, in logarithmic scale. Even if the above feature is explicitly mentioned in the current NAS Commentary (item F of Section E2 – AISI 2016), there are no provisions/guidelines on how to take it into account when designing short-to-intermediate angle columns by means of the DSM.

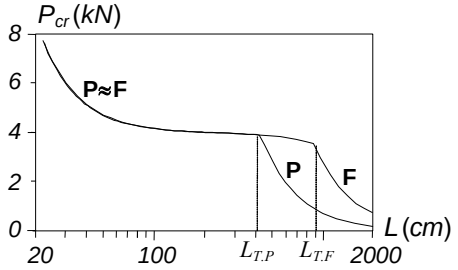

Figure 1. Typical "signature" curves P_{cr} vs. L of fixed-ended (F) and pin-ended (P) columns

Since the flexural-torsional buckling deformations occurring in equal-leg angle columns are predominantly torsional and very similar/akin to local deformations, these columns have been said, erroneously, to fail in local-global interactive modes, thus explaining why their design on the basis local strength concepts is still implicitly prescribed by AISI (2016). Indeed, up to a couple of years ago, the most successful attempts to develop an efficient DSM-based approach to design equal-leg short-to-intermediate angle columns, developed by Young (2004 – F columns), Rasmussen (2006 – P columns) and Silvestre *et al*. (2013 – F and P columns), involve the use of either (i) the currently codified DSM

[2] Recall that the failure loads of the longer angle columns, which exhibit a "trivial" minor-axis flexural buckling behavior, are adequately predicted by the currently codified DSM global strength curve.

[3] It should be mentioned that these two support conditions only differ in the restraint of the end-section minor-axis flexural rotations, which are either fully restrained (fixed end) or completely free (pinned end) – in both cases, the columns are fixed-ended with respect to major-axis flexure and have the (secondary) warping of their end cross-sections fully restrained. In the experimental studies, warping fixity is achieved by attaching thick/rigid plates to the column end cross-sections and the pin-ended support conditions correspond to "cylindrical hinges".

column local design curve or (ii) a slightly modified (empirically) version of this curve. This situation was altered by Dinis *et al.* (2012) and Mesacasa *et al.* (2014), who provided clear numerical evidence that the column failure stems from the interaction between major-axis flexural-torsional and minor-axis flexural buckling – a kind of unique global coupling phenomenon that (i) does not involve local deformations, (ii) is highly sensitive to the "sign" of the minor-axis flexural initial geometrical imperfections and (iii) exhibits very clear length-dependent characteristics. These findings led Dinis & Camotim (2015) to develop a novel DSM-based design approach, based on flexural-torsional strength curves (instead of local ones) and valid for both fixed-ended and pin-ended short-to-intermediate angle columns, which was shown to predict quite well the available failure loads (experimental and/or numerical) – the reliability assessment prescribed by AISI (2016) (see Section 1.1) shows that the LRFD resistance factors associated with this design approach never fall below ϕ_c=0.85. In order to improve its user-friendliness, without sacrificing efficiency, the design approach was slightly simplified a bit later (Dinis & Camotim 2016) – this last version is the one considered in this work.

After collecting the available experimental failure loads, concerning both fixed-ended and pin-ended short-to-intermediate angle columns, the paper demonstrates that the currently DSM local-global interactive strength curve is unable to estimate them adequately, thus justifying the need for the codification of a novel DSM-based design approach able to handle such columns. Then, a brief overview of the structural reasoning behind the DSM-based design approach proposed by Dinis & Camotim (2016) is presented, paying special attention to (i) the replacement of local buckling concepts by flexural-torsional ones, (ii) the length-dependence of the strength curves involved and (iii) the need to use different strength curves to design otherwise identical fixed-ended and pin-ended columns. Next, the quality (accuracy and reliability) of the failure load estimates provided by the proposed DSM-based design approach is assessed through the prediction of the above experimental failure load data and also a fairly large number of numerical failure loads (obtained in previous works). It is confirmed that the LRFD resistance factor recommended in AISI (2016) for compression members (ϕ_c=0.85) can be adopted also for angle columns designed with this DSM-based approach. Finally, the paper presents and discusses a few numerical examples, which illustrate the application of the proposed DSM-based design approach and evidence its advantages and benefits, when compared with the currently codified one, making it possible to conclude that it deserves to be considered for inclusion in a future version of the North American Specification for the Design of Cold-Formed Steel Structural Members.

1.1 Load and Resistance Factor Design (LRFD)

According to Section K2.1.1 of AISI (2016), the LFRD resistance factor is given by

$$\phi_c = C_\phi \left(M_m F_m P_m \right) e^{-\beta_0 \sqrt{V_M^2 + V_F^2 + C_P V_P^2 + V_Q^2}} \tag{1}$$

where (i) C_ϕ=1.52 (calibration coefficient for LRFD), (ii) M_m=1.10 and F_m=1.00 (taken from Table K2.1.1-1 of the specification) are the material and fabrication factor mean values, (iii) β_0 is the target reliability value (β_0=2.5 for structural members in LRFD), (iv) V_M=0.10 and V_F=0.05 (also taken from Table K2.1.1-1) are the material and fabrication factors, (v) V_Q=0.21 is the coefficient of variation of the load effect, and (vi) C_p is a correction factor dependent on the number of tests. The P_m and V_p values are the mean and coefficient of variation of the "exact" (experimental/numerical)-to-predicted failure load ratios. As already mentioned, the value recommended for compression members is ϕ_c=0.85, regardless of the column failure mode nature – however, lower ϕ_c values have been are reported for equal-leg angle columns (*e.g.*, Ganesan & Moen 2012).

2. Experimental Failure Load Data of Cold-Formed Steel Angle Columns

The experimental failure loads, previously collected by Dinis & Camotim (2016) concern (i) 37 fixed-ended columns, tested by Popovic *et al.* (1999), Young (2004) and Mesacasa Jr. (2012), and (ii) 50 pin-ended columns, tested by Wilhoite *et al.* (1984), Popovic *et al.* (1999), Chodraui *et al.* (2006), Maia *et al.* (2008)[4] and Landesmann *et al.* (2016) – it is worth noting that 4 fixed and 5 pin-ended columns tested by Popovic *et al.* (1999) were excluded from this investigation, because they did not fail in flexural-torsional modes, (their lengths are located in the P_{cr} (L) curve descending branch, *i.e.*, they buckle in minor-axis flexural modes). Note that, for equal angles with sharp corners, the maximum column length lying on the signature curve plateau (length associated with coincident major-axis flexural-torsional and minor-axis flexural critical buckling load), termed L=$L_{T.F}$ and L=$L_{T.P}$ (see Fig. 1), are given by the expressions

$$L_{T.F} = b\sqrt{\frac{\pi^2\, K_F}{6}} \qquad \text{with} \quad K_F = (1+\nu)\left[2.25\left(\frac{b}{t}\right)^2 - 4.0\right] \tag{2a}$$

$$L_{T.P} = b\sqrt{\frac{\pi^2\, K_P}{6}} \qquad \text{with} \quad K_P = (1+\nu)\left[0.5125\left(\frac{b}{t}\right)^2 - 4.0\right], \tag{2b}$$

where b and t are the leg mid-line width and thickness, and ν is Poisson's ratio.

The columns selected exhibit leg width, thickness and length values in the following ranges: (i) fixed-ended columns with $71.1 \geq b \geq 47.7$ *mm*, $4.7 \geq t \geq 1.2$ *mm*, $60.7 \geq b/t \geq 10.1$, $3500 \geq L \geq 150$ *mm* and (ii) pin-ended columns with $90.8 \geq b \geq 47.7$ *mm*, $4.7 \geq t \geq 1.6$ *mm*, $58.2 \geq b/t \geq 10.1$, $1636 \geq L \geq 285$ *mm*. Therefore, a total of 87 experimental failure loads are available, a number deemed acceptable to assess the merits of DSM-based design

[4] It is worth noting that none of the 4 fixed-ended columns tested by Maia *et al.* (2008) was included in the failure load data, since the ultimate strengths reported do not seem plausible – they are lower than those reported by those authors for pin-ended columns with almost identical geometrical and material characteristics.

approaches. Table 1 provides the numbers and origins of the available test results concerning fixed-ended and pin-ended columns (the measured specimen dimensions and steel properties can be found in the appropriate references) and Fig. 2 plots their failure-to-yield load ratios P_u/P against the column flexural-torsional (critical) slenderness λ_{ft}.

Table 1. Experimental failure loads test concerning fixed and pin-ended equal-leg angle columns

	Fixed-ended columns		Pin-ended columns	
Tests			Wilhoite *et al.* (1984)	8
	Popovic *et al.* (1999)	11	Popovic *et al.* (1999)	13
	Young (2004)	21	Chodraui *et al.* (2006)	4
	Mesacasa Jr. (2012)	5	Maia *et al.*(2008)	5
			Landesmann *et al.*(2016)	20
Total		37		50

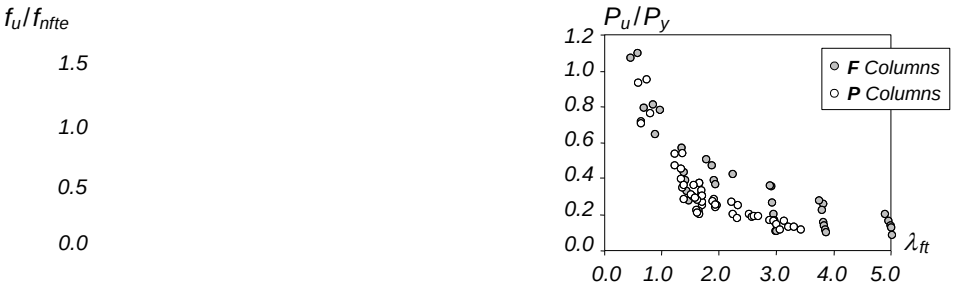

Figure 2. Plots P_u/P_y vs. λ_{ft} concerning the fixed-ended (F) and pin-ended (P) column tests

3. Direct Strength Method (DSM) Design

The currently codified DSM strength/design curves for cold-formed steel columns are defined by "Winter-type" expressions that (i) were calibrated against fairly large numbers of experimental and/or numerical failure loads and (ii) provide safe and accurate ultimate strength estimates associated with local, distortional, global and local-global interactive failures on the sole basis of the elastic critical buckling and squash loads. In the context of this investigation on angle columns the relevant nominal strengths are P_{nl} (local), P_{ne} (global) and P_{nle} (local-global), given by (AISI 2016)

$$P_{nl} = \begin{cases} P_y & \text{if} \quad \lambda_l \le 0.776 \\ P_y \left(\frac{P_{crl}}{P_y}\right)^{0.4} \left[1 - 0.15\left(\frac{P_{crl}}{P_y}\right)^{0.4}\right] & \text{if} \quad \lambda_l > 0.776 \end{cases} \quad \text{with } \lambda_l = (P_y/P_{crl})^{0.5}, \quad (3)$$

$$P_{ne}=\begin{cases} P_y\left(0.658^{\lambda_c^2}\right) & if \quad \lambda_c \le 1.5 \\ P_y\left(\dfrac{0.877}{\lambda_c^2}\right) & if \quad \lambda_c > 1.5 \end{cases} \quad \text{with } \lambda_c=(P_y/P_{cre})^{0.5}, \quad (4)$$

$$P_{nle}=\begin{cases} P_{ne} & if \quad \lambda_{le} \le 0.776 \\ P_{ne}\left(\dfrac{P_{crl}}{P_{ne}}\right)^{0.4}\left[1-0.15\left(\dfrac{P_{crl}}{P_{ne}}\right)^{0.4}\right] & if \quad \lambda_{le} > 0.776 \end{cases} \quad \text{with } \lambda_{le}=(P_{ne}/P_{crl})^{0.5}, \quad (5)$$

where (i) λ_l, λ_c and λ_{le} are the local, global and interactive slenderness values, (ii) P_{crl} and P_{cre} are the column local and global buckling loads, and (iii) P_y is the squash load – they are calculated on the basis of the gross cross-section area (A_g) and the elastic buckling (f_{cr}) or the steel yield (f_y) stresses.

Since the concept of pre-qualification was removed from latest specification version (AISI 2016), P_{nle} is the only viable option to predict the ultimate strength of concentrically loaded short-to-intermediate angle columns, assumed to fail in "local"-global modes. Note that such an approach is conceptually wrong, since the above columns effectively buckle and fail in major-axis flexural-torsional modes. Moreover, the mechanical characteristics of those flexural-torsional modes have been found to vary significantly along the $P_{cr}(L)$ curve horizontal plateau (Dinis *et al*. 2012).

An average designer intending to use Eq. (5), which involves also Eq. (4), must calculate the column local (P_{crl}) and global (P_{cre}) elastic critical buckling loads. Assuming access to rigorous software and no particular knowledge on angle column stability, he/she is faced with different options on how to calculate the above buckling loads. Indeed, since the deformation patterns associated with local and flexural-torsional torsional buckling are very similar (both designations are often used), it may happen that P_{crl} is calculated either (i) by using a software tool, which actually provides the column flexural-torsional buckling load (P_{crfl}), or (ii) through the codified expression for the local buckling of unstiffened uniformly compressed elements (outstand walls), which reads

$$f_{bl}=0.43\,\frac{\pi^2\,E}{12(1-\nu^2)}\left(\frac{t}{w}\right)^2 \quad , \quad (6)$$

where $w=b-(r_i+t/2)$ is the leg flat width (r_i the inside bend radius) – then, one is led to $P_{crl}=f_{bl}\times A_g$. On the other hand, since the flexural-torsional buckling mode has a global nature, it may also happen that the average designer considers P_{cre} associated with either the major-axis flexural-torsional (F_MT –incorrectly) or the minor-axis flexural (F_m – correctly) buckling mode. Table 2 lists the conceivable options of the average designer to calculate P_{crl} and P_{cre} in the context of the DSM-based design of short-to-intermediate equal-leg angle columns.

Table 2. Conceivable options to calculate P_{crl} and P_{cre}, in the context of the determination of P_{nle}

Option	1	2	3
P_{crl}	$F_M T$	L	L
P_{cre}	F_m	F_m	$F_M T$

It should be pointed out that the major-axis flexural-torsional (f_{crft}) and minor-axis flexural (f_{bfm}) buckling stresses are provided by the "exact" expressions (Dinis & Camotim 2015)

$$f_{crft} = \frac{4}{5}\left(f_{bt} + f_{bf} - \sqrt{(f_{bt} + f_{bf})^2 - 2.5\, f_{bt}\, f_{bf}} \right) \tag{7a}$$

$$f_{bt} = G\frac{t^2}{b^2} + \pi^2 \frac{E\, t^2}{12(L/2)^2} \tag{7b}$$

$$f_{bf} = \pi^2 \frac{E\, b^2}{6(L/2)^2} \tag{7c}$$

$$f_{bfm} = \begin{cases} \pi^2 \dfrac{E\, b^2}{24(L/2)^2} & for\ fixed\text{-}ended\ columns \\ \pi^2 \dfrac{E\, b^2}{24\, L^2} & for\ pin\text{-}ended\ columns \end{cases}, \tag{8}$$

where (i) E and $G=E/[2(1+\nu)]$ are the steel Young's and shear moduli, and (ii) f_{bt} and f_{bf} are the (pin-ended and fixed-ended) angle column pure torsional and major-axis flexural buckling stresses, respectively.

Figs. 3(a)-(c) plot, against the interactive slenderness λ_{le}, the failure-to-predicted load ratios P_u/P_{nle} of the whole set of experimental failure loads gathered in Section 2 – P_{nle} are failure load estimates provided by the currently codified DSM local-global interactive design curves, for the three options defined in Table 2. The figures show also the P_u/P_{nle} averages, standard deviations and maximum/minimum values, as well as the resistance factors ϕ_c they lead to. The observation of these results prompts the following remarks:

(i) The three options provide an unsatisfactory estimation of the experimental column failure loads, which constitutes clear evidence that AISI (2016) does not cover adequately the DSM design of short-to-intermediate equal-leg angle columns.

(ii) The first two options provide similarly (highly) unsafe failure load predictions: average/minimum values of 0.74/0.35 (Option 1) and 0.72/0.35 (Option 2). Note that these predictions are particularly unsatisfactory for the P columns: (ii_1) averages of 0.68 and 0.66 (predictions become gradually worse as λ_{le} increases), and (ii_2) only a few P_{nle} estimates are safe and accurate ($P_u/P_{nle} \geq 1.00$) for Options 1 and 2 – to be exact, 8 out of 50 for both options.

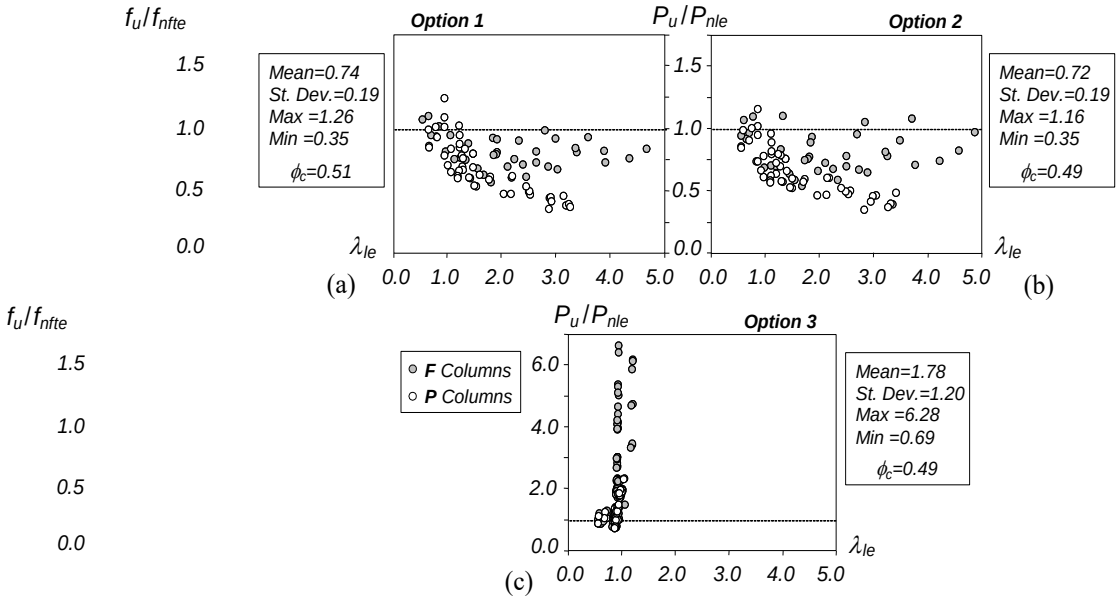

Figure 3. Plots P_u/P_{nle} vs. λ_{le} concerning the F and P column experimental failure loads, provided by the DSM local-global interactive design curves associated with Options (a) 1, (b) 2 and (c) 3

(iii) On the other hand, Option 3 lead to overly safe column failure load estimates: average/maximum values of 1.78/6.28[5]. The best predictions concern now the P columns: average/maximum values of 1.26/2.29 and only 16 estimates are such that $1.00 > P_u/P_{nle} \geq 0.73$ (just 5 F column estimates with $P_u/P_{nle}<1.00$). It is worth noting that even higher average/maximum values (3.02/9.01) were obtained in a similar investigation carried out by Ganesan & Moen (2012)[6].

(iv) The poor estimation quality achieved of by three options is reflected by the quite low resistance factors: the best value is ϕ_c=0.51, obtained with Option 1, which is still very far from the recommended value (ϕ_c=0.85 – AISI 2016).

Recalling that this work deals exclusively with short-to-intermediate angle columns (those buckling in major-axis flexural-torsional modes), it is worth looking at the interactive slenderness ranges covered, for the test specimens considered, when each option is adopted. While Options 1 and 2 lead to similar and quite wide ranges ($0.52 \leq \lambda_{le} \leq 4.62$ and $0.48 \leq \lambda_{le} \leq 4.77$, respectively), Option 3 leads to a fairly short low range ($0.47 \leq \lambda_{le} \leq 1.16$)

[5] Since local and flexural-torsional buckling are basically two designations of the same instability phenomenon, the corresponding critical buckling loads are invariably almost coincident, which explains why all the columns exhibit similar slenderness values that are always very close to 1.0 (see Fig. 3(c)).

[6] Although the authors provide no clear information on the definition/calculation of the local and global critical buckling loads, the results obtained strongly suggest that they have adopted Option 3.

– the last range merely reflects the fact that Option 3 is based on an interaction between two buckling phenomena that are, effectively, the same one (viewed first as "local" and then as "global"). On the other hand, the quite wide slenderness range covered when adopting Options 1 or 2 (or also the proposed DSM design approach, addressed next in Section 4) is due to the fact that (i) the "local"/flexural-torsional buckling load is practically uniform along the short-to-intermediate column length range (except in very short columns, P_{crl} – or, to be precise, P_{crft} – corresponds to an almost horizontal $P(L)$ curve "plateau") while and (ii) the global strength P_{ne} decreases quite fast within that same length range. Moreover, this fact implies that a short column exhibits a higher λ_{le} value than its otherwise identical longer counterparts – this surprising (counterintuitive) feature, which was first pointed out by Landesmann *et al.* (2016), is illustrated in Fig. 4. This explains the apparent lack of correlation between the angle column lengths and λ_{le} values.

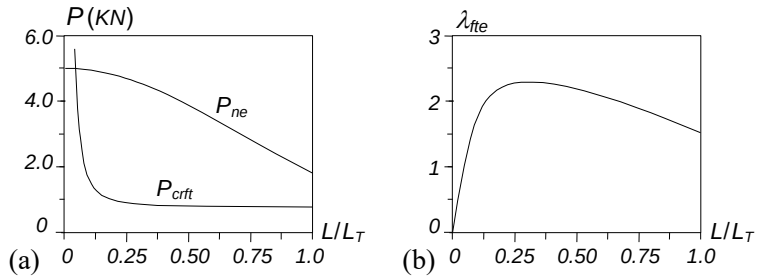

Figure 4. Illustrative plots showing the variation, with $L \leq L_T$, of (a) P_{ne} and P_{crft}, and (b) λ_{fte}

4. Proposed DSM-Based Design Approach

The DSM design of cold-formed steel angle columns has attracted the attention of a few researchers in the past, namely Young (2004), Rasmussen (2006) and Silvestre *et al*. (2013). Even if the approaches proposed by these researchers were found to predict the available failure load data quite reasonably, the fact they are mostly empirical led the authors (Dinis & Camotim 2015) to develop a rational (taking into account the problem mechanics) DSM-based design approach able to handle fixed-ended and pin-ended columns – this approach was subsequently slightly modified/simplified by Landesmann *et al.* (2016) and Dinis & Camotim (2016). Its main features are the following:

(i) Based on the fact that most short-to-intermediate angle columns fail in interactive modes combing major-axis flexural-torsional and minor-axis flexural deformations.

(ii) Involves the use of the currently codified DSM global design curve (P_{ne}) and a set of genuine flexural-torsional strength curves (P_{nft}), obtained by analyzing columns with fully prevented minor-axis bending displacements. These strength curves, valid for both fixed-ended and pin-ended columns, make it possible to capture the length-dependent column post-critical strength (it progressively drops as the length increases along the $P_{cr}(L)$ curve "horizontal plateau").

(iii) The effective centroid shift effects (Young & Rasmussen 1999), heavily influencing the pin-ended column failure loads (not the fixed-ended ones), are included in the design approach through a coefficient β, which is also length-dependent.

Therefore, the proposed DSM-based design approach requires (i) developing a set of genuine flexural-torsional strength curves, covering adequately the whole $P_{cr}(L)$ curve plateau, and (ii) quantifying the effective centroid shift effects (in pin-ended columns), which is done through a "reduction factor" based on the relation between the elastic post-buckling strengths of otherwise identical pin-ended and fixed-ended columns. The main concepts and procedures involved in the performance of these tasks are addressed next.

4.1 Flexural-torsional strength curves

Fig. 5(a) plots, against λ_{ft}, the P_u/P_y values corresponding to the flexural-torsional failure load data obtained by Dinis & Camotim (2015) for columns with the minor-axis bending displacements fully prevented – also shown is the current DSM local strength curve. Due to the huge "vertical dispersion" of the P_u/P_y values, it is clear that no single Winter-type curve is able to predict adequately (safely and accurately) all of them. It is also clear that a large fraction of those values fall well below the current DSM local strength curve. The above "vertical dispersion" is closely linked to the column length. Indeed, the P_u/P_y values gradually drop as L increases along the $P_{cr}(L)$ curve "plateau", which is in line with the findings obtained for the unrestrained columns (Dinis & Camotim 2015). Fig. 5(b) illustrates the length-dependence of the restrained column post-buckling strength: the four elastic equilibrium paths displayed, concerning columns with increasing lengths L_1-L_4, evidence a very clear post-critical strength drop.

An in-depth investigation on the column pure flexural-torsional behavior unveiled that the participation of major-axis flexure in the column critical buckling mode (i) increases gradually with L (see Fig. 5(b)) and (ii) can be directly related to the difference between the pure torsional (f_{bt}) and flexural-torsional (f_{crft} – critical) buckling stresses, given by Eqs. (7). In view of these findings, it was decided to group the columns according to the

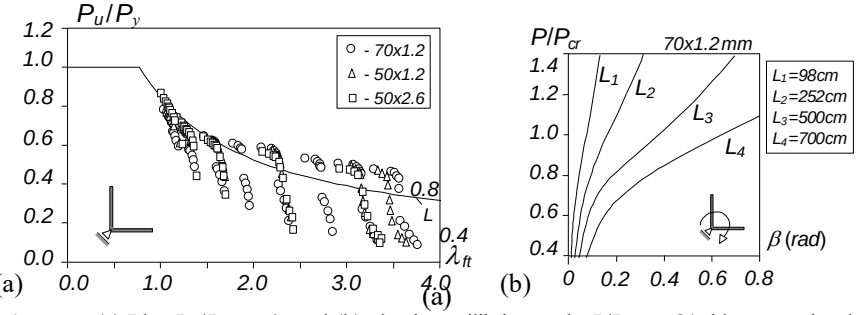

Figure 5. (a) Plot P_u/P_y vs. λ_{ft} and (b) elastic equilibrium paths P/P_{cr} vs. β (mid-span torsional rotation) of restrained 70×1.2*mm* columns with lengths L=98,252,500,700*cm*

percentage difference between f_{bt} and f_{crft}, *i.e.*, to $\Delta_f=[(f_{bt}-f_{crft})/f_{bt}]\times 100$ – this parameter quantifies the relative importance of major-axis flexure in the flexural-torsional buckling behavior and, therefore, is ideally suited to quantify the length-dependence of the column post-critical strength along the $P_{cr}(L)$ curve plateau[7]. Then, the proposed flexural-torsional strength curves (P_{nft}) are defined by "Winter-type" expressions incorporating parameter Δ_f to account for the length-dependence – they read (Dinis & Camotim 2016)

$$P_{nfte}=\begin{cases} P_{ne} & if \quad \lambda_{fte}\le\left(0.5+\sqrt{0.25-b}\right)^{\frac{1}{2a}} \\ P_{ne}\left(\dfrac{P_{crft}}{P_{ne}}\right)^{a}\left[1-b\left(\dfrac{P_{crft}}{P_{ne}}\right)^{a}\right] & if \quad \lambda_{fte}>\left(0.5+\sqrt{0.25-b}\right)^{\frac{1}{2a}} \end{cases} \tag{9}$$

$$a=\begin{cases} 0.19\,\Delta_f+0.4 & if \quad \Delta_f<3 \\ 0.97 & if \quad \Delta_f\ge 3 \end{cases} \qquad b=\begin{cases} 0.014\,\Delta_f+0.15 & if \quad \Delta_f\le 7 \\ 0.248 & if \quad \Delta_f>7 \end{cases}, \tag{10}$$

where each combination of parameters a and b leads to a different curve – the length-dependence is captured through these two parameters, both expressed in terms of Δ_f. Note that a=0.4 and b=0.15 are adopted for Δ_f=0, which implies that Eq. (9) coincides with the current DSM local strength curve (Eq. (3)) for columns with f_{bt}/f_{crft} very close to 1.00.

It was found that the proposed P_{nft} strength curve set is able to capture the "vertical dispersion" of the numerical failure load data displayed in Fig. 5(a). Figs. 6(a)-(b) show two flexural-torsional strength curves, obtained from Eq. (9) and associated with Δ_f=1.80 and Δ_f=7.20, which illustrate this assertion: the numerical failure loads of the columns exhibiting those Δ_f values are fairly well predicted by them – naturally, the prediction quality varies with Δ_f (in this case, it is better for Δ_f=7.20).

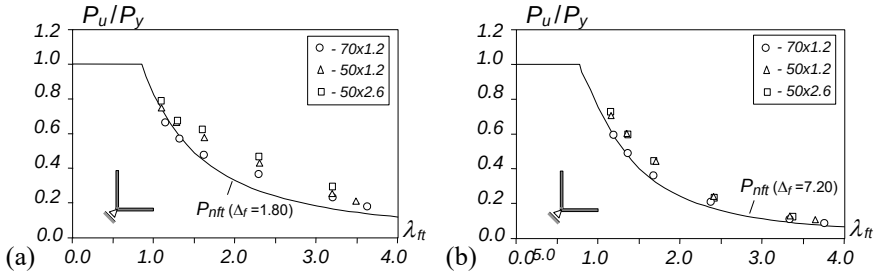

Figure 6. Plots of P_u/P_y vs. λ_{ft} and proposed flexural-torsional (P_{nft}) strength curves for columns with minor-axis bending displacements fully prevented such that (a) Δ_f=1.80 and (b) Δ_f=7.20

[7] This expression was proposed by Landesmann *et al.* (2016) and differs slightly from the original Δ_f definition put forward by Dinis & Camotim (2015).

Recalling that the mechanical reasoning behind the DSM design approach is based on the fact that the columns fail in global-global interactive modes, combing major-axis flexural-torsional and minor-axis flexural deformations, it is now possible to obtain the nominal strength against the above failures (P_{nfte}) of fixed-ended (F) short-to-intermediate angle columns. It suffices to replace P_y by P_{ne} (nominal failure load provided by the current DSM global design curve) in Eq. (9) – the ensuing strength curve set is expressed in terms of the "interactive" slenderness $\lambda_{fte}=(P_{ne}/P_{crft})^{0.5}$.

4.2 Reduction parameter β

The next step consists of finding a length-dependent "reduction parameter" β that, when multiplied by the F column nominal strengths P_{nfte}, provides their pin-ended (P) column counterparts. The procedure adopted to search for this parameter is based on an "elastic reduction factor" concept and involves the following steps:

(i) Perform elastic post-buckling analyses of identical F and P columns (same f_{bt}/f_{crft} ratio, *i.e.*, Δ_f value), both containing critical-mode initial geometrical imperfections with amplitude $L/1000$, and record the evolution, as the applied load increases, of the maximum longitudinal normal stresses at mid-span (f_{max}) – the P vs. f_{max} curves of the F and P columns associated with Δ_f=0.16 are displayed in Fig. 7(a).

(ii) Calculate, for any given f_{max} value, the ratio between the F and P column applied loads causing it (P_F and P_P) – note that difference between P_F and P_P stems solely from the effective centroid shift effects, which make the interaction with minor-axis flexural buckling much more pronounced in the P column. If f_{max} is equal to the column yield stress ($f_{max}=f_y$), the corresponding P_P/P_F ratio provides the strength reduction parameter at the column "elastic limit state".

(iii) Assume that the above P_P/P_F ratio is a good enough approximation of the sought strength reduction parameter at the column elastic-plastic failure (β) – in other words, assume that $\beta \approx P_P/P_F$.

(iv) Take f_{max} as the column global nominal strength f_{ne}, thus implying that its interactive slenderness reads $\lambda_{fte}=(f_{max}/f_{crft})^{0.5}$ and enabling the establishment of a relationship

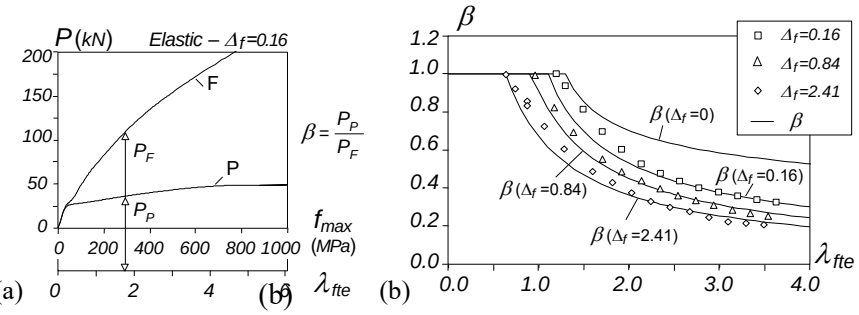

Figure 7. (a) P vs. f_{max} curves of F and P columns with Δ_f=0.16, (b) numerically obtained β values, plotted against λ_{fte}, and proposed $\beta(\lambda_{fte})$ curves relating P and F columns with Δ_f=0.16, 0.84, 2.41

between β and λ_{fte}. Then, it is possible to obtain a set of length-dependent $\beta(\lambda_{fte})$ curves, one per Δ_f value – Fig. 7(b) shows the $\beta(\lambda_{fte})$ curves of columns exhibiting Δ_f=0.16, Δ_f=0.84 and Δ_f=2.41. The differences between the curves clearly evidence the length-dependence of $\beta(\lambda_{fte}) - \beta$ decreases substantially as L (*i.e.*, Δ_f) increases.

(v) Using a trial-and-error curve-fitting procedure, search for Winter-type expressions relating β to λ_{fte} – the simpler output of this search is (Dinis & Camotim 2016)

$$\beta = \frac{0.68}{(\lambda_{fte} - c)^d} \leq 1 \tag{11}$$

$$c = -0.2\,\Delta_f + 0.55 \qquad\qquad d = 0.08\,\Delta_f + 0.72 \quad . \tag{12}$$

4.3 DSM design proposal

Combining now (i) the strength curves for fixed-ended columns, obtained in Section 4.1 and consisting of Eqs. (9) with P_y replaced by P_{ne}, and (ii) the reduction parameter β, just obtained in Section 4.2, it is possible to propose DSM-based strength curves providing nominal failure loads (P_{nfte}) of short-to-intermediate fixed-ended and pin-ended angle columns, which fail in global-global interactive modes combining torsional rotations with major- and minor-axis translations – they are defined by the expressions

$$P_{nfte} = \begin{cases} \beta \cdot P_{ne} & \text{if} \quad \lambda_{fte} \leq \left(0.5 + \sqrt{0.25 - b}\right)^{\frac{1}{2a}} \\ \beta \cdot P_{ne} \left(\dfrac{P_{crft}}{P_{ne}}\right)^a \left[1 - b \left(\dfrac{P_{crft}}{P_{ne}}\right)^a\right] & \text{if} \quad \lambda_{fte} > \left(0.5 + \sqrt{0.25 - b}\right)^{\frac{1}{2a}} \end{cases} \tag{13}$$

$$\beta = \begin{cases} 1 & \textit{for fixed - ended columns} \\ \dfrac{0.68}{(\lambda_{fte} - c)^d} \leq 1 & \textit{for pin - ended columns} \end{cases} \tag{14}$$

where (i) a, b and c, d are given by Eqs. (10) and (12), (ii) $\lambda_{fte}=(P_{ne}/P_{crft})^{0.5}$ is the interactive slenderness and (iii) P_{ne} is obtained from the currently codified DSM global design curve (Eq. (4)).

4.4 Merit assessment

The above DSM-based strength curves provide quite accurate and reliable failure load predictions. Figs. 8(a)-(b) plot, against λ_{fte}, the failure-to-predicted load ratios (P_u/P_{nfte}) concerning (i) the experimental failure loads presented in Section 2 (37 F and 50 P columns) and (ii) the numerical failure loads (337 F and 296 P columns) obtained by the

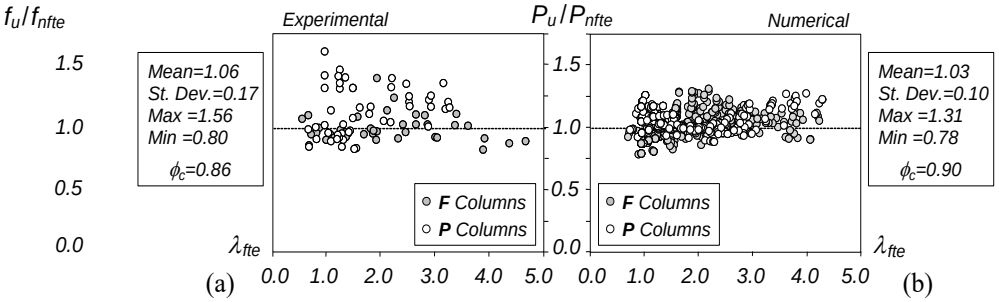

Figure 8. P_u/P_{nfte} vs. λ_{fte} plots: (a) experimental and (b) numerical F and P column failure loads

authors and gathered in Dinis & Camotim (2016). The observation of the P_u/P_{nfte} averages, standard deviations and maximum/minimum values, as well as the corresponding ϕ_c values, clearly shows the quality of the performance indicators concerning the proposed DSM-based design approach – in particular, it should be emphasized that ϕ_c=0.85 can now be used for cold-formed steel angle columns, regardless of their lengths.

In view of the above results, a DSM-based design proposal for fixed-ended and pin-ended equal-leg angle columns can be formulated, establishing that the nominal strength is $P_n=min\{P_{ne}; P_{nfte}\}$, where P_{ne} and P_{nfte} are provided by the current DSM global design curve and Eqs. (13)-(14), respectively – the former applies to the longer columns, which buckle and fail in pure minor-axis flexural modes. In view of the results reported in this work, the authors believe that this design proposal is ready for codification.

5. Illustration

In order to illustrate the application and benefits of the proposed DSM-based design approach to estimate the failure loads of short-to-intermediate cold-formed steel equal-leg angle columns, numerical results are presented and discussed in this section. They concern F and P columns exhibiting the geometries and material properties of specimens tested by Young (2004) and Landesmann *et al.* (2016), respectively – these geometries and material properties are given in Table 3, while Table 4 provides the corresponding buckling and squash loads (P_{bt}, P_{bf}, P_{crft}, P_{bfm}, P_{bl}, P_y). Tables 5 and 6 show the column failure loads and their estimates provided using (i) the DSM local-global interactive design curve (P_{nle}), according to the three options defined in Table 2, and (ii) the proposed DSM-based design approach (P_{nfte}) – these tables also include relevant quantities involved in the failure load estimation, namely the slenderness values (λ_c, λ_{le} or λ_{fte}), the nominal global strength (P_{ne}) and the Δ_f, a, b, c, d, β parameter values. After observing these results, it can be readily concluded that the P_{nfte} values constitute safe and fairly accurate failure load estimates (P_u/P_{nfte}=1.12 and P_u/P_{nfte}=1.15, respectively for the F and P columns), which clearly outperform their P_{nle} counterparts: they are either (i) substantially unsafe, when Options 1 or 2 are adopted (P_u/P_{nle}=0.81 and P_u/P_{nle}=0.37, for Option 1, and P_u/P_{nfte}=0.79 and P_u/P_{nfte}=0.37, for Option 2) or (ii) overly safe

Table 3. F and P specimen geometry, material properties, buckling and squash loads (dimensions in *mm*, stresses in *MPa*)

	F column (Young 2004)		P column (Landesmann *et al*. 2016)	
Geometrical properties	$b\times t\times L$ 71.1×1.17×2500	A_g=166.6 r_i=2.6 w=67.9	$b\times t\times L$ 90.8×1.56×897	A_g=283.3 r_i=1.55 w=88.5
Material properties	E=208×10^3 G=80×10^3	f_y=550	E=205×10^3 G=78.8×10^3	f_y=305

Table 4: F and P specimen buckling and squash loads (stresses in *MPa*, loads in *kN*)

	F column (Young 2004)		P column (Landesmann *et al*. 2016)	
Torsional buckling	f_{bt}=**21.8** (Eq. 7b)	$P_{bt} = A_g \times f_{bt}$=**3.6**	f_{bt}=**25.3** (Eq. 7b)	$P_{bt} = A_g \times f_{bt}$=**7.2**
Major-axis flexural buckling	f_{bf}=**1107.4** (Eq. 7c)	$P_{bf} = A_g \times f_{bf}$ =**184.4**	f_{bf}=**13824.4** (Eq. 7c)	$P_{bf} = A_g \times f_{bf}$ =**3916.8**
Flexural-torsional buckling	f_{crft}=**21.7** (Eq. 7a)	$P_{crft} = A_g \times f_{crft}$=**3.6**	f_{crft}=**25.3** (Eq. 7a)	$P_{crft} = A_g \times f_{crft}$=**7.2**
Minor axis flexural buckling	f_{bfm}=**276.9** (Eq. 8)	$P_{bfm} = A_g \times f_{bfm}$=**46.1**	f_{bfm}=**864.0** (Eq. 8)	$P_{bfm} = A_g \times f_{bfm}$=**244.8**
Local buckling	f_{bl}=**24.0** (Eq. 6)	$P_{bl} = A_g \times f_{bl}$=**4.0**	f_{bl}=**24.8** (Eq. 6)	$P_{bl} = A_g \times f_{bl}$=**7.0**
Squash load		$P_y = A_g \times f_y$ =**91.6**		$P_y = A_g \times f_y$ =**87.0**

Table 5: F column specimen failure load (Young 2004) and its DSM estimates (dimensions in *mm*, stresses in *MPa*, loads in *kN*)

	P_{nle}				P_{nfte}		
	Option	1	2	3			
Flexural critical load	P_{cre}	**46.1** (P_{bfm})	**46.1** (P_{bfm})	**3.6** (P_{crft})	Flexural critical load	P_{cre}	**46.1** (P_{bfm})
Global slenderness	$\lambda_c=(P_y/P_{cre})^{0.5}$	**1.41**	**1.41**	**5.08**	Global slenderness	$\lambda_c=(P_y/P_{cre})^{0.5}$	**1.41**
Nominal global load	P_{ne} (Eq. 4)	**39.9**	**39.9**	**3.1**	Nominal global load	P_{ne} (Eq. 4)	**39.9**
Local critical load	P_{crl}	**3.6** (P_{crft})	**4.0** (P_{bl})	**4.0** (P_{bl})	Flexural-torsional critical load	P_{crft}	**3.6** (P_{crft})
Interactive slenderness	$\lambda_{le}=(P_{ne}/P_{crl})^{0.5}$	**3.32**	**3.16**	**0.89**	Interactive slenderness	$\lambda_{fte}=(P_{ne}/P_{crft})^{0.5}$	**3.32**
Nominal strength	P_{nle} (Eq. 5)	**14.4**	**14.9**	**2.9**	Nominal strength	Δ_f	**0.74**
						a (Eq. 10)	**0.54**
						b (Eq. 10)	**0.16**
						β (Eq. 14)	**1.00**
						P_{nfte} (Eq. 13)	**10.4**
Failure load	P_u	**11.6**			Failure load	P_u	**11.6**
Load ratio	$\frac{P_u}{P_{nle}}$	**0.81**	**0.78**	**4.01**	Load ratio	$\frac{P_u}{P_{nfte}}$	**1.12**

Table 6. P column specimen failure load (Landesmann *et al*. 2016) and its DSM estimates (dimensions in *mm*, stresses in *MPa*, loads in *kN*)

	P_{nle}				P_{nfte}		
	Option	1	2	3			
Flexural critical load	P_{cre}	**244.8** (P_{bfm})	**244.8** (P_{bfm})	**7.0** (P_{crft})	Flexural critical load	P_{cre}	**244.8** (P_{bfm})
Global slenderness	$\lambda_c=(P_y/P_{cre})^{0.5}$	**0.59**	**0.59**	**3.47**	Global slenderness	$\lambda_c=(P_y/P_{cre})^{0.5}$	**0.59**
Nominal global load	P_{ne} (Eq. 4)	**74.4**	**74.4**	**6.3**	Nominal global load	P_{ne} (Eq. 4)	**74.4**
Local critical load	P_{crl}	**7.2** (P_{crft})	**7.0** (P_{bl})	**7.0** (P_{bl})	Flexural-torsional critical load	P_{crft}	**7.2** (P_{crft})
Interactive slenderness	$\lambda_{le}=(P_{ne}/P_{crl})^{0.5}$	**3.22**	**3.26**	**0.95**	Interactive slenderness	$\lambda_{fte}=(P_{ne}/P_{crft})^{0.5}$	**3.22**
Nominal strength	P_{nle} (Eq.5)	**27.5**	**27.3**	**5.5**	Nominal strength	Δ_f	**0.07**
						a (Eq. 10)	**0.41**
						b (Eq. 10)	**0.15**
						c (Eq. 12)	**0.54**
						d (Eq. 12)	**0.73**
						β (Eq. 14)	**0.33**
						P_{nfte} (Eq. 13)	**8.9**
Failure load	P_u	**10.2**			Failure load	P_u	**10.2**
Load ratio	$\frac{P_u}{P_{nle}}$	**0.37**	**0.37**	**1.83**	Load ratio	$\frac{P_u}{P_{nfte}}$	**1.15**

for Option 3 (P_u/P_{nfte}=4.01 and P_u/P_{nfte}=1.83). Since Option 1 corresponds to the most rational use of the currently codified DSM design curves (in the authors' opinion, of course), only this option is considered in the remainder of this section – nevertheless, note that the conclusions drawn would still applicable to Option 2, which is fairly similar to Option 1 (only Option 3 should be definitely removed from the picture).

In order to further illustrate and compare the failure load estimation quality achieved when employing Option 1 and the proposed approach, a representative sample of 12 (6 F + 6 P) columns are considered, covering a wide slenderness range and including the F and P columns dealt with above in this section. Their (experimental) failure loads and respective estimates (P_{nle} and P_{nfte}) are provided in Table 7, together with the specimen (i) origins and dimensions (b, t, L) and (ii) slenderness values ($\lambda_{le}=\lambda_{fte}$). The observation of the P_u/P_{nle} values confirms the poor estimation quality, regardless of the slenderness value – indeed, all the specimen failure loads are overestimated by amounts that range from 9% to 43% (F columns) or 14% to 65% (P columns). Moreover, the comparison between the P_u/P_{nfte} and P_u/P_{nle} values provides very clear evidence on how sharply the former outperform the latter. Indeed, the P_{nfte} estimates are never worse than the P_{nle} ones: they are (i) safe, for six column (by amounts going up to 41%, in F columns, and to 29%, in P columns), (ii) less unsafe, for five columns (differences between 1% and 64%, and worst overestimation of 15%) and (iii) equally unsafe, for one column (overestimation of 14%).

Table 7. Selected specimen geometries, slenderness values, failure loads and respective P_{nle} (Option 1) and P_{nfte} estimates (dimensions in *mm*, loads in *kN*)

	Specimen $b \times t \times L$	P_u	λ_{le}	P_{nle}	$\frac{P_u}{P_{nle}}$	λ_{fte}	P_{nfte}	$\frac{P_u}{P_{nfte}}$
F1	70.8×1.50×3500 Young (2004)	11.6	1.87	14.2	**0.81**	1.87	8.2	**1.41**
F2	70.8×1.50×250 Young (2004)	39.9	2.96	43.8	**0.91**	2.96	43.4	**0.92**
F3	71.1×1.17×1000 Young (2004)	18.8	4.62	22.6	**0.83**	4.62	21.1	**0.89**
F4	71.1×1.17×2500 Young (2004)	11.6	3.32	14.4	**0.81**	3.32	10.4	**1.12**
F5	71.1×1.88×3000 Young (2004)	14.9	1.75	26.0	**0.57**	1.75	14.8	**1.01**
F6	59.0×2.00×1800 Mesacasa Jr. (2012)	20.8	1.63	33.2	**0.63**	1.63	21.8	**0.95**
P1	80.7×1.56×908 Landesmann *et al.* (2016)	9.1	2.83	25.8	**0.35**	2.83	9.2	**0.99**
P2	60.7×1.58×596 Landesmann *et al.* (2016)	11.9	2.13	25.3	**0.47**	2.13	11.6	**1.02**
P3	90.8×1.56×897 Landesmann *et al.* (2016)	10.2	3.22	27.5	**0.37**	3.22	8.9	**1.15**
P4	67.5×3.00×1227 Wilhoite *et al.* (1984)	56.8	1.18	66.5	**0.85**	1.18	44.0	**1.29**
P5	47.7×4.70×490 Popovic *et al* (1999)	122.2	0.62	142.0	**0.86**	0.62	142.0	**0.86**
P6	58.8×2.40×1550 Chodraui *et al* (2006)	21.4	0.91	26.9	**0.79**	0.91	21.6	**0.99**

6. Conclusion

This paper championed a proposal for the codification of a DSM design approach for concentrically loaded cold-formed steel equal-leg angle short-to-intermediate columns, originally developed by Dinis & Camotim (2015) and subsequently slightly modified and simplified by Landesmann *et al.* (2016) and Dinis & Camotim (2016). Initially, the available experimental failure load data, concerning fixed-ended and pin-ended columns with several geometries (cross-section dimensions and length) and reported by various researchers, were collected and characterized. Then, it was shown that the DSM design curves included in the latest version of the North American Specification for the Design of Cold-Formed Steel Structural Members (AISI 2016), supposedly covering short-to-intermediate angle columns (assumed to fail in local-global interactive modes), are unable to predict adequately the failure loads of such columns – indeed, the three conceivable usages of the above DSM design curves lead to LRFD resistance factors well below ϕ_c=0.85, value recommended in AISI (2016) for compression members. Then, the paper (i) presented a brief overview of the proposed novel DSM design approach, including the mechanical reasoning behind the key concepts and procedures involved, and (ii) assessed

its merits (safety, accuracy and reliability), through (ii_1) the quality of the experimental and numerical failure load predictions, and (ii_2) the determination of the LRFD resistance factors they lead to. In particular, it was shown that ϕ_c=0.85 can also be adopted for short-to-intermediate angle columns, thus making sure ensuring that this value really applies to all compression members, as prescribed in AISI (2016). Finally, the paper illustrated the application and quantified the benefits of the proposed DSM design approach – detailed numerical results concerning the calculation of failure load estimates in fixed-ended and pin-ended columns were presented and discussed.

In the authors' opinion, it was clearly shown that, in the specific context of concentrically loaded cold-formed steel equal-leg angle short-to-intermediate columns, the proposed DSM-based design approach is ready to be considered for codification, by replacing the currently codified DSM local-global interactive design, which very often leads to either unsafe or excessively safe failure load predictions (depending on how it is interpreted).

References

AISI (American Iron and Steel Institute) (2012). *North American Specification* (NAS) *for the Design of Cold-Formed Steel Structural Members* (AISI-S100-12), Washington DC.

AISI (American Iron and Steel Institute) (2016). *North American Specification* (NAS) *for the Design of Cold-Formed Steel Structural Members* (AISI-S100-16), Washington DC.

Camotim D, Dinis PB and Martins AD (2016). Direct Strength Method (DSM) – a general approach for the design of cold-formed steel structures, *Recent Trends in Cold-Formed Steel Construction*, C. Yu (ed.), Woodhead Publishing (Amsterdam), 69-105.

Chodraui GMB, Shifferaw Y, Malite M and Schafer BW (2006). Cold-formed steel angles under axial compression, *Proceedings of 18th International Specialty Conference on Cold-Formed Steel Structures* (Orlando, 26-27/10), R. LaBoube, W.W. Yu (eds.), 285-300.

Dinis PB and Camotim D (2015). A novel DSM-based approach for the rational design of fixed-ended and pin-ended short-to-intermediate thin-walled angle columns, *Thin-Walled Structures*, **87**(February), 158-182.

Dinis PB and Camotim D (2016). Proposal for the codification of a DSM design approach for cold-formed steel short-to-intermediate angle columns, *Proceedings of Wei-Wen Yu International Specialty Conference on Cold-Formed Steel Structures* (CCFSS 2016 – Baltimore, 9-10/11) R. LaBoube, W.-W. Yu (eds.), 155-171.

Dinis PB, Camotim D and Silvestre N (2012). On the mechanics of angle column instability, *Thin-Walled Structures*, **52**(March), 80-89.

Ganesan K and Moen CD (2012). LRFD resistance factor for cold-formed steel compression members, *Journal of Constructional Steel Research*, **72**(May), 261-266.

Landesmann A, Camotim D, Dinis PB and Cruz R (2016). Short-to-intermediate slender pin-ended cold-formed steel equal-leg angle columns: experimental investigation, numerical simulation and DSM design, *Engineering Structures*, **132**(February), 471-493.

Maia WF, Neto JM and Malite M (2008). Stability of cold-formed steel simple and lipped angles under compression, *Proceedings of 19th International Specialty Conference on Cold-Formed Steel Structures* (St. Louis, 26-27/10), R. LaBoube, W.W. Yu (eds.), 111-125.

Mesacasa Jr. E (2012). *Structural Behavior and Design of Cold-Formed Steel Angle Columns*, MASc Thesis in Structural Engineering, School of Engineering at São Carlos, University of São Paulo, Brazil. (Portuguese)

Mesacasa Jr. E, Dinis PB, Camotim D and Malite M (2014). Mode interaction and imperfection-sensitivity in thin-walled equal-leg angle columns, *Thin-Walled Structures*, **81**(August), 138-149.

Popovic D, Hancock GJ and Rasmussen KJR (1999). Axial compression tests of cold-formed angles, *Journal of Structural Engineering* (ASCE), **125**(5), 515-523.

Rasmussen KJR (2006). Design of slender angle section beam-columns by the direct strength method, *Journal of Structural Engineering* (ASCE), **132**(2), 204-211.

Schafer BW (2008). Review: the direct strength method of cold-formed steel member design, *Journal of Constructional Steel Research*, **64**(7-8), 766-778.

Silvestre N, Dinis PB and Camotim D (2013). Developments on the design of cold-formed steel angles, *Journal of Structural Engineering* (ASCE), **139**(5), 680-694.

Wilhoite GM, Zandonini R and Zavelani A (1984). Behaviour and strength of angles in compression: an experimental investigation, *Proceedings of ASCE Annual Convention and Structures Congress* (San Francisco, 1-3/10).

Young B (2004). Tests and design of fixed-ended cold-formed steel plain angle columns, *Journal of Structural Engineering* (ASCE), **130**(12), 1931-1940.

Young B and Rasmussen KJR (1999). Shift of effective centroid in channel columns, *Journal of Structural Engineering* (ASCE), **125**(5), 524-531.